Physicochem. Probl. Miner. Process., 62(3), 2026, 224722

http://www.journalssystem.com/ppmp

Physicochemical Problems of Mineral Processing

ISSN 1643-1049
© Wroclaw University of Science and Technology

Mineralogical characteristic and environment-friendly leaching tests for a lateritic gold ore

Zhugao Yu, Daixin Sun, Xian Xie, Qilin Zhai, Fengcui Cao, Xiong Tong

Faculty of Land Resources Engineering, Kunming University of Science and Technology, Kunming 650000, China
National Local Joint Engineering Research Center for Green Utilization of Metal Tailings Resources, Kunming 650093, China

Corresponding author: kgxianxie@126.com (Xian Xie)

Abstract: A systematic process mineralogy study and non-cyanide leaching tests were conducted on a lateritic gold ore. Process mineralogy analysis shows that the iron content in the ore reaches 42.60%, with a gold grade of 21.20 g/t. Gold occurs mainly as free and semi-exposed native gold (76.46%) and limonite-encapsulated gold (23.18%). The disseminated grain size of gold is fine. Gold is predominantly encapsulated by limonite and associated with pyrite, with only a small portion hosted in pyrite. Although the ore contains a high proportion of free and semi exposed gold, it exhibits poor leachability under conventional leaching conditions, as the fine gold particles are embedded and encapsulated within limonite. In consideration of the ore properties and green environmental protection requirements, a clean gold extraction process—fine grinding–ethylenediaminetetraacetic acid (EDTA) pretreatment leaching–environmentally friendly leaching agent Jinchan (JC) leaching–activated carbon adsorption—was developed. Through system optimization, the optimal process parameters were determined: grinding fineness of 85% at −0.074 mm, 0.25 g/L EDTA pretreatment for 12 h, JC leaching agent dosage of 5 g/L, 2.5 g/L CaO to adjust the pH to 12, and leaching time of 36 h. Under these conditions, the gold leaching rate increased to 97.17%, and the gold grade of the tailings decreased to 0.60 g/t. This study provides a reliable technical scheme and theoretical foundation for the efficient and environmentally friendly leaching of lateritic refractory gold deposits, as well as the green and economic development of similar mineral resources.

Keywords: lateritic gold, non-cyanide leaching, environment-friendly leaching gold, process mineralogy

1. Introduction

The readily extractable, high-grade gold ore deposits worldwide are steadily being depleted, making the utilization and efficient recovery of complex, refractory gold ores increasingly imperative (Li et al., 2024; Zhang et al., 2022). Lateritic gold deposits are one of emerging as a significant source of precious metals, driven by growing demand and surging gold prices, presenting opportunities for economic processing (Iglesias-Martínez et al., 2024). Lateritic gold deposits form through the physical accumulation and biogeochemical redistribution of primary ore during weathering processes. Native gold is the primary gold mineral, occurring as fine-grained particles. It is predominantly disseminated as intergranular and fracture gold within limonite, or is adsorbed onto or encapsulated by clay minerals and iron oxides. Consequently, complete liberation is difficult to achieve, which prevents direct contact with leaching solutions and consequently reduces gold extraction efficiency (Liu et al., 2023; Varajão et al., 2000).

In the gold leaching process, the cyanidation method has long dominated the global gold extraction industry. Cyanide possesses high toxicity and is subject to stringent environmental regulations. Therefore, the development of green gold leaching processes to replace cyanidation has become a research hotspot in the field of gold leaching (Shafiei et al., 2025; Zhong et al., 2025). In recent years, a variety of environmentally friendly gold leaching systems have been gradually promoted for industrial

DOI: 10.37190/ppmp/224722

application, such as thiourea, thiosulfate, polysulfide, and halide leaching systems. However, although thiourea exhibits a high leaching efficiency and low environmental pollution, it suffers from drawbacks including a high cost, potential carcinogenicity, and poor chemical stability (Hilson & Monhemius, 2006). Thiosulfate and polysulfide tend to form a passivation film on mineral surfaces via by-product formation, thereby reducing leaching efficiency. The thiosulfate system also requires ammonia catalysis, and the subsequent process for gold recovery from leachate remains immature (Niu et al., 2023). In addition, the halide system causes severe equipment corrosion, and gold halide complex ions exhibit low stability in aqueous solution (Zhang et al., 2022). Therefore, many research institutions and enterprises have conducted research and development on novel eco-friendly gold leaching agents, among which JC is a high-performance environmentally benign gold leaching agent (Ma et al., 2025; Nair et al., 2024; Shi et al., 2025). Such reagents typically use urea, ferricyanide, and alkali metal salts as the main components. Under high-temperature conditions, the synergistic effect of these components enables the efficient dissolution of gold in non-cyanide systems, demonstrating promising application prospects. Guo et al. (2022) investigated the leaching of Carlin-type gold concentrate using a novel environmentally friendly gold extractant JC. Under optimized process conditions, the gold leaching rate could reach 90.8%. Guo et al. (2015) compared the leaching performance of JC and sodium cyanide for a gold ore in Laos. The results demonstrated that the gold leaching rates of JC and sodium cyanide were 97.3% and 96.2%, respectively, under identical process parameters. Previous studies have confirmed that the toxicity of the residue after JC leaching is much lower than that from conventional cyanidation leaching. Compared with other environmentally benign gold leaching systems such as thiosulfate and iodide, JC exhibits more consistent reagent consumption and demonstrates superior selectivity for fine-grained gold present in laterite-type gold ores. Meanwhile, this lixiviant avoids the conventional oxidant demands and ammonia catalysis used in thiosulfate systems.

JC consists of a mixture of sodium cyanurate, basic thiourea, and stabilisers (Zhang et al., 2022). Its primary active ingredient is sodium cyanurate (chemical formula: $C_6H_3O_3N_6Na_3$). The cyanide-like group (CN^-) within sodium cyanurate is bound by strong covalent bonds, remaining in a stable complexed state under normal conditions rather than as free cyanide ions. This is the primary reason why JC, although detectable in trace amounts of cyanide ions, exhibits non-toxic or low-toxicity properties towards humans and other organisms (Guo et al., 2022; Pengzhi et al., 2015). The primary gold leaching reaction equation for JC is shown in Eq. (1):

$$8C_6H_3O_3N_6Na_3 + 4Au + 2H_2O + O_2 \rightarrow 4\ NaAu(C_6H_3O_3N_6Na_2)_2 + 4NaOH \quad (1)$$

The laterite-type gold ore used in the test is a primary ore deposit formed through weathering, erosion, transportation, and deposition. Visually, the majority of the ore exhibits a brown colouration, with brown interspersed with light yellowish-copper tones. It is primarily composed of limonite, with a small proportion consisting of pyrite. Against this backdrop, analytical techniques, including X-ray fluorescence spectroscopy (XRF), inductively coupled plasma mass spectrometry (ICP-MS), inductively coupled plasma optical emission spectroscopy (ICP-OES/AES), atomic absorption spectroscopy (AAS), and polarizing microscopy, were employed to conduct a systematic study on the process mineralogy of refractory gold deposits in lateritic ores. Building upon this foundation, a non-cyanide, environmentally friendly leaching process utilizing the JC was developed. This work provides both theoretical underpinnings and practical guidance for the green and efficient extraction of such refractory gold resources.

2. Materials and methods

2.1. Materials

The lateritic gold ore used in the test was sourced from an overseas mine. It belongs to the orebody of primary ore formed via weathering-denudation and transportation-deposition processes. Visual observation of the ore showed that most of the ore samples exhibited a brown or brownish colour with faint brassy luster, and were predominantly composed of limonite; a small portion of the ore samples, by contrast, consisted mainly of pyrite. The ore was dried, crushed to a −2 mm size fraction and thoroughly homogenized, after which process mineralogy tests and leaching tests were carried out.

Sodium hydroxide (NaOH) and calcium oxide (CaO) were used to adjust the pH of the slurry. In addition, the leaching agents potassium permanganate ($KMnO_4$), ammonium chloride (NH_4Cl), lead nitrate ($Pb(NO_3)_2$), ethylenediaminetetraacetic acid (EDTA), and citric acid ($C_6H_8O_7$) were all analytical-grade reagents supplied by McLean Biochemical Technology Co., Ltd. (Shanghai, China). Hydrogen peroxide (H_2O_2), obtained from Guanjia Chemical Reagent Co., Ltd. (Hunan, China), was of industrial grade. The leaching agent JC was supplied by Guangxi Senhe Mining Technology Co., Ltd. (Guangxi, China).

2.2. Methods

2.2.1. Process mineralogy study

To comprehensively characterize the mineralogical properties of gold in the raw ore, the present study employed X-ray fluorescence spectrometry (XRF), inductively coupled plasma mass spectrometry (ICP-MS), inductively coupled plasma atomic emission spectrometry (ICP-OES/AES), and atomic absorption spectrometry (AAS) along with other analytical techniques to conduct quantitative analyses of the major, minor, and trace elements. These analyses were further utilized to evaluate the ore grade and guide subsequent mineral processing tests. The mineral composition, dissemination relationship and degree of dissociation were systematically characterized using a mineral dissociation analysis system, a polarizing microscope, an electron probe microanalyzer and a scanning electron microscope. In addition, the purpose of chemical phase analysis for gold is to determine the content of elements in various phases within the sample, as well as to provide the required material composition and the occurrence states of elements in the ore for geochemical anomaly assessment, geological investigation, deposit evaluation, and mineral processing test research. The contents of the target components in the sample are determined via chemical methods following selective dissolution and separation.

Given the characteristics of low gold content and fine dissemination size in the sample, a combined method of manual gravity separation-enrichment and microscopic observation was employed to accurately analyze the particle size distribution and morphology of the gold minerals. The specific process is as follows: first, heavy minerals were obtained via manual elutriation; subsequently, the ore was observed under a polarizing microscope, and gold-bearing mineral particles were manually picked out and mounted on a glass slide; finally, a calibrated eyepiece micrometer was used to measure the particle size, with classification carried out based on the visual morphological characteristics of the particles. By observing a sufficient number of particles, the statistical representativeness of the acquired data was ensured, while the dissociation behavior and surface morphological characteristics of gold-bearing minerals were effectively elucidated.

2.2.2. Leaching experiments

The main procedure of the leaching test is as follows: a 50 g gold ore sample is weighed, ground to the specified particle size, and transferred into a 500 mL beaker. 200 mL of deionized water is added to the beaker to prepare a slurry with a liquid-solid ratio of 4:1 (pulp concentration 20%). After adding the leaching aid, the beaker is placed in a heat-collecting constant-temperature heating magnetic stirrer. The pretreatment test is conducted at a temperature of 25 ± 1 °C, atmospheric pressure (101.325 kPa, with no additional oxygen or inert gas introduced), and a stirring rate of 500 r/min. After pretreatment, the pulp pH was adjusted to an appropriate value using a pH regulator, and a leaching agent was then added to conduct the leaching test. After leaching was completed, solid–liquid separation was performed by vacuum filtration. The leaching residue was thoroughly washed with deionized water and dried to constant weight in an oven at 100 °C. The pregnant leach solution was adsorbed with activated carbon to obtain loaded carbon and barren solution. The experimental procedure is illustrated in Fig. 1. The gold grade of the dried leaching residue was determined by atomic absorption spectrometry (AAS), and the gold leaching rate was calculated accordingly. All test results are presented as the average of triplicate parallel experiments. The formula for calculating the gold leaching rate (εAu) is given in Eq. 2:

$$\varepsilon = \left(1 - \frac{m \times a}{m_0 \times a_0}\right) \times 100\% \quad (2)$$

ε is the gold leaching rate (%); m_0 and a_0 are the mass (g) and gold grade (g/t) of the ore sample, respectively, and m and a are the mass (g) and gold grade (g/t) of the leaching residue, respectively.

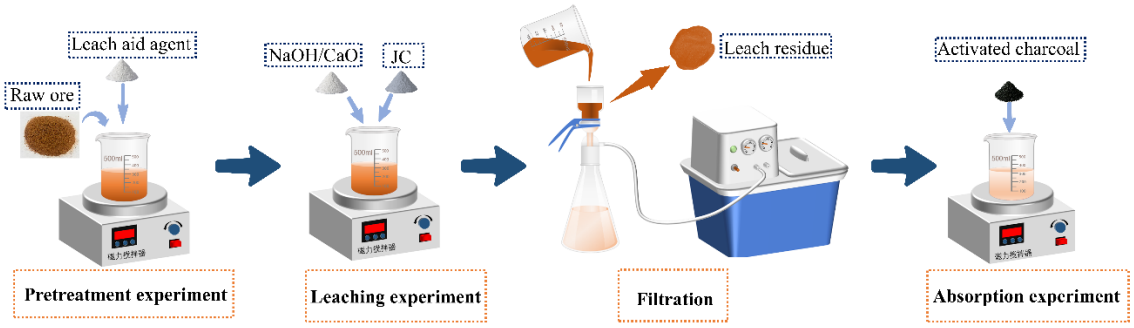

Fig. 1. Leaching experiment process

3. Results and discussion

3.1. Process mineralogy results

3.1.1. Chemical multielement analysis

The results of chemical multi-element analysis for a refractory gold-silver ore with an iron content of 42.60% from overseas are presented in Table 1. The valuable elements in this ore are mainly gold and silver, with a gold grade of 21.20 g/t and a silver grade of 67.30 g/t. Both gold and silver possess high recovery potential, while the ore also contains trace amounts of lead, copper and zinc. Its gangue components are dominated by silica, alumina and carbonate minerals, and the ore exhibits a low content of the harmful element arsenic—a feature that is favorable for subsequent beneficiation processes.

Table 1. Results of multi-element analysis of ore chemistry

Elements	Au	Elements	SiO_2	Cu	Pb	Zn	TFe	S
Concentration(g/t)	21.20	Concentratio (%)	11.14	0.45	1.59	0.22	42.60	2.08
Elements	Ag	Elements	Al_2O_3	CaO	MgO	K_2O	Na_2O	As
Concentration(g/t)	67.30	Concentratio (%)	4.12	2.01	1.72	0.54	0.09	0.36

3.1.2 Chemical multielement analysis

Polished thin-section observation, multi-element chemical analysis, and X-ray powder diffraction (XRD) analysis revealed that the ore contains 13 mineral species, belonging to the categories of native elements, sulfides, oxides, silicates, carbonates, and arsenate sulfates. Specifically, native elements are present at approximately 20 g/t, sulfides account for 7.5%, oxides make up 73.4%, silicates constitute 8.7%, and carbonates represent 7.8%; arsenates and sulfates are only occasionally observed. The primary ore minerals include native gold (electrum), limonite, plus minor amounts of chalcopyrite, covellite, and pyrite, while the dominant gangue minerals are quartz, dolomite, sericite, and kaolinite.

3.1.3. Phase analysis of ore gold

The results of ore gold phase analysis are shown in Table 2.

Table 2. Gold chemical phase analysis results

Phase	Free and semi-free natural gold	Carbonate-encapsulated gold	Cu-Pb-Zn sulfides encapsulates gold	Limonite-encapsulated gold	Quartz and silicates encapsulates gold	Pyrite-encapsulated gold	Total
Concentration (g/t)	16.21	0.03	0.013	4.914	0.013	0.02	21.20
Relative content (%)	76.46	0.14	0.06	23.18	0.06	0.09	100.00

The results of chemical phase analysis presented in Table 2 indicate that free and semi-free gold accounts for 76.46%, limonite-encapsulated gold accounts for 23.18%, carbonate-encapsulated gold accounts for 0.14%, gold encapsulated by Cu-Pb-Zn sulfides accounts for 0.06%, gold encapsulated by quartz and silicates accounts for 0.06%, and pyrite-encapsulated gold accounts for 0.09%. Gold in this ore is therefore dominated by free and semi-free forms, a morphological characteristic that is conducive to gold beneficiation.

3.1.4. Dissemination characteristics of minerals

Exploring the characteristics of mineral dissemination provides a scientific basis for the efficient, economical and clean utilization of mineral resources (Ma et al., 2024; Zhang et al., 2024). By revealing key information including the spatial distribution, particle size, morphology, paragenetic associations of minerals within the ore as well as their correlations with gangue minerals, this approach offers direct evidence for guiding beneficiation process design, optimizing mining and ore blending schemes, and assessing the recovery potential of associated elements.

3.1.4.1. Natural gold and electrum

Natural gold and electrum are the principal ore minerals present in the ore, with a gold grade of 20 g/t. Artificial heavy mineral concentrates were subjected to elutriation prior to observation under a binocular microscope; the concentrates exhibited a golden-yellow color. Owing to the frequent adhesion of limonite to their surfaces, the gold grains appear dark golden-yellow with a strong metallic luster. Gold occurs predominantly in granular form, with a minor amount of dendritic and flaky morphologies, as illustrated in Fig. 2a. Polarized light microscopy observations showed that the target mineral was predominantly encapsulated by limonite and pyrite, and disseminated between pyrite grains, as illustrated in Figs. 2b and 2c. A small fraction was encapsulated within quartz, limonite, and pyrite. As presented in Fig. 2d, the mineral exhibited a wide particle size range of <0.01–0.5 mm, with a fine-grained dissemination as the dominant occurrence state. Its minimum particle size was less than 0.005 mm, and the maximum particle size reached approximately 0.5 mm.

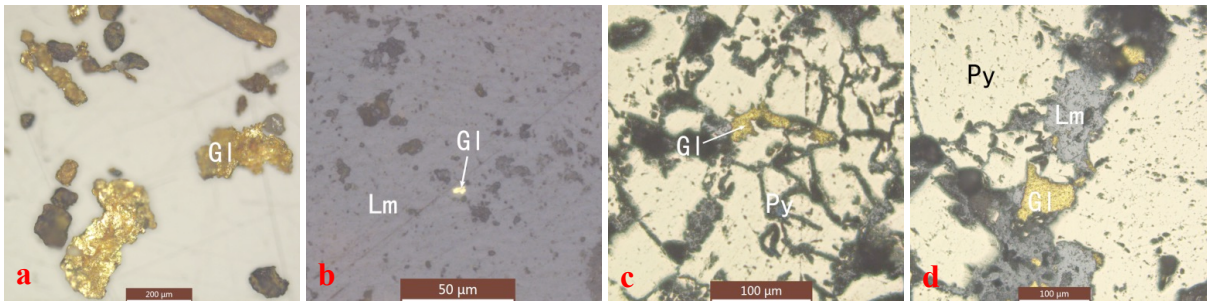

Fig. 2. Microphotographs A plate-like, granular native gold (Gl) selected from artificial heavy sand； Micrograph b Micro-fine natural gold (Gl) is wrapped in limonite (Lm)； Microphotographs of c-pyrite (Py) particles between the fissure gold (Gl)； Microphotographs d Natural gold (Gl) is associated with pyrite (Py) and limonite (Lm).

SEM-EDS analysis revealed that the gold content in natural gold grains ranged from 77.43 to 92.02%, while the silver content ranged from 5.22 to 92.02%. Trace amounts of Fe and O were also detected, with the detailed results presented in Table 3 and Fig. 3.

Table 3. Energy spectrum analysis results of natural gold and electrum

Elements (%) / Dot mark	Fe	Ag	Au	O	Minerals
6504 (Fig.3a)	8.69	5.22	86.10	-	Electrum
6512 (Fig.3b)	5.87	16.70	77.43	-	Electrum
6526 (Fig.3c)	1.19	7.43	90.53	0.85	Native gold
6527 (Fig.3c)	1.14	5.68	92.02	1.16	Electrum

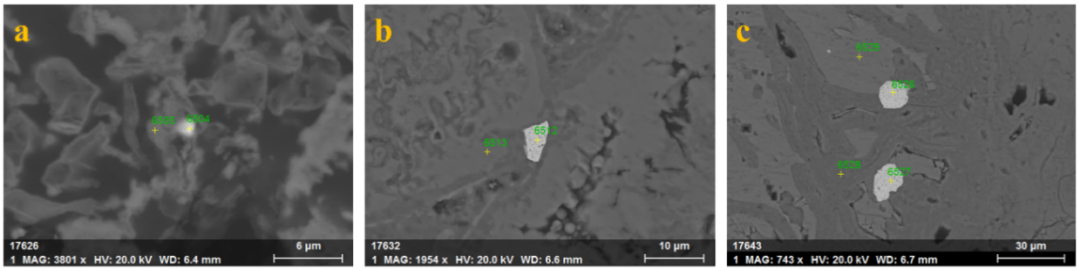

Fig. 3. Backscattered electron diagram of natural gold

3.1.4.2. Natural silver

Natural silver was identified via electron microscopy; it occurred sporadically within the ore and exhibited a particle size of less than 0.01 mm. EDS analysis indicated that the natural silver had a chemical composition of 83.78% Ag, 4.16% Fe, 1.45% S, and 10.61% O. The relevant results are presented in Table 4 and Fig. 4.

Table 4. Energy spectrum analysis results of natural silver

Elements (%) / Dot mark	Fe	Ag	Au	O
6493	4.16	83.78	1.45	10.61

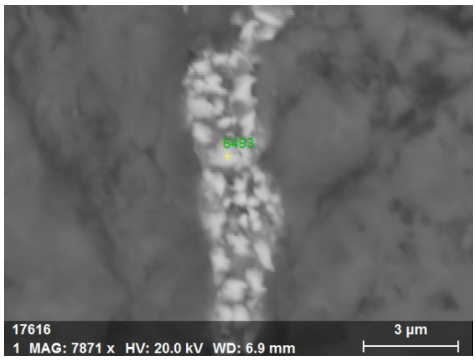

Fig. 4. Backscattered electron diagram of natural silver

4. Pyrite

Pyrite is one of the major ore minerals. It occurs as hypidiomorphic granular and xenomorphic granular aggregates, which are relatively concentrated in certain ore domains. Minor residual grains are distributed within limonite and closely associated with it, as illustrated in Fig. 5a. A small number of pyrite grains are also associated with magnetite, chalcopyrite and covellite, as shown in Fig. 5b. The particle size of pyrite generally ranges from 0.01 to 0.8 mm, with the maximum reaching tens of millimeters.

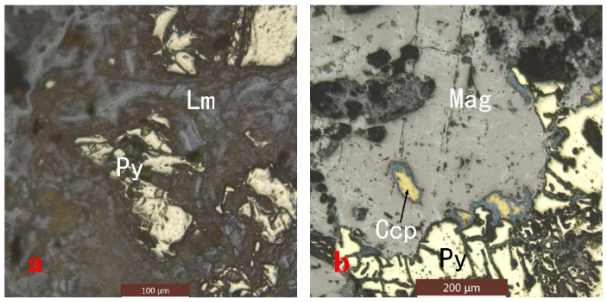

Fig. 5. Microscopic photograph a) It-shaped granular pyrite (Py) is associated with limonite (Lm); Microscopic image b) Pyrite (Py) is associated with magnetite (Mag)

5. Oxide

Limonite is one of the principal ore minerals. Its monomineralic grains occur as cryptocrystalline and micritic varieties, while its aggregates exhibit granular textures. Limonite predominantly forms via the alteration of pyrite, typically occurring as pyrite pseudomorphs with colloform and crustose habits, and frequently retains pyrite relics. A small amount of gangue minerals, including muscovite and quartz, are encapsulated within limonite, which exhibits a close paragenetic association with native gold. Native gold is mainly encapsulated in limonite. In terms of grain size distribution, limonite generally ranges from 0.001 to 0.6 mm in particle size, as illustrated in Fig. 6a.

Quartz is among the minor gangue minerals in the ore system. It typically occurs in granular and clastic forms, either occurring in association with limonite and kaolinite or being encapsulated within limonite. This mineral exhibits an uneven distribution throughout the ore, with its particle size ranging from 0.01 to 0.5 mm, as illustrated in Fig. 6b. Magnetite occurs as an accessory ore mineral; it is granular in morphology, closely associated with pyrite, and observed locally, with a particle size ranging from 0.04 to 0.3 mm, as shown in Fig. 6c.Sericite (muscovite) is one of the minor gangue minerals in the ore system. It exhibits a microscopic scaly and flaky morphology; most aggregates occur as relatively concentrated vein-like distributions, whereas a small portion is scattered within limonite. Its particle size ranges from 0.01 to 0.4 mm, as illustrated in Fig. 6d. Kaolinite is one of the minor gangue minerals, characterized by a microscopic scaly-cryptocrystalline morphology. It is mostly impregnated with limonite and has a particle size of less than 0.1 mm, as illustrated in Fig. 6e. Dolomite represents the primary gangue mineral, exhibiting a euhedral-subhedral granular texture. It occurs predominantly in concentrated distributions with a particle size ranging from 0.01 to 0.7 mm, as shown in Fig. 6f. Arsenopyrite is classified as one of the accessory minerals, featuring an irregular granular shape. It occurs in intergrowth with limonite and has a particle size between 0.03 and 0.6 mm, as depicted in Fig. 6g. Gypsum is an occasional mineral with a platy morphology. It is commonly encapsulated within limonite and has a particle size ranging from 0.05 to 0.2 mm, as presented in Fig. 6h.

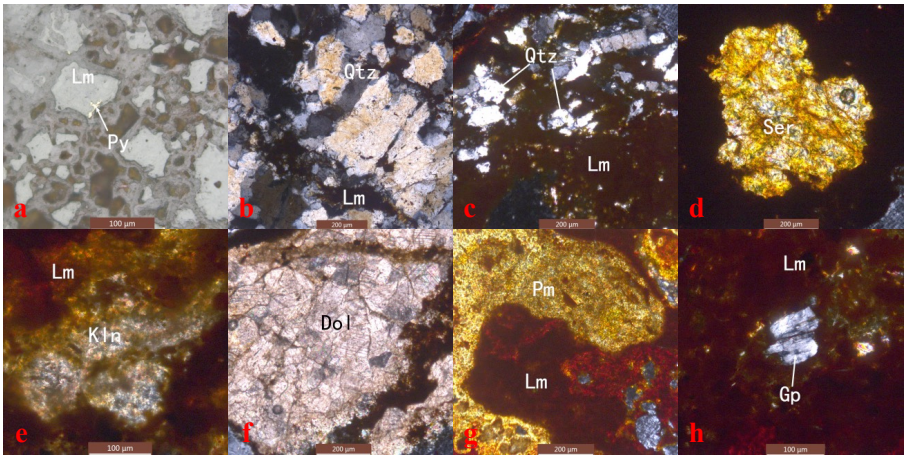

Fig. 6. Microscopic photograph a) Residual pyrite (Py) is seen in the granular limonite (Lm); Microscopic photograph b) It-shaped granular quartz (Qtz) is associated with limonite (Lm); Microphotographs of c) quartz (Qtz) wrapped in limonite (Lm); Microscopic photographs of d) sericite (Ser) aggregation distribution; Microscopic photographs of e) kaolinite (Kln) was disseminated by limonite (Lm); Microscopic photo f) dolomite (Dol) aggregation distribution; Microscopic photographs of g) show that g-arsenopyrite (Pm) is associated with limonite (Lm); Microscopic photographs of h) limonite (Lm) wrapped in gypsum (Gp)

5.1. Leaching test results

5.1.1. Direct leaching test results

Based on the ore properties, the primary gold-bearing component in the ore occurs as native gold and electrum. To evaluate the leaching difficulty of the ore and ascertain the leachability of its constituent minerals, a 50 g sample of crushed ore (particle size: −2 mm) was weighed and placed in a beaker. The leaching experiment was conducted in a heat-collecting constant-temperature heating magnetic stirrer, at a temperature of 25 ± 1 °C

and a stirring speed of 500 r/min. The liquid-to-solid ratio was set at 4:1, and the initial pH of the slurry was adjusted to 12 using CaO and NaOH, respectively. Subsequently, a dosage of 5 g/L JC and NaCN reagent was added for the direct leaching test. The schematic diagram of the experimental procedure is presented in Fig. 7a, and the corresponding test results are illustrated in Fig. 7b.

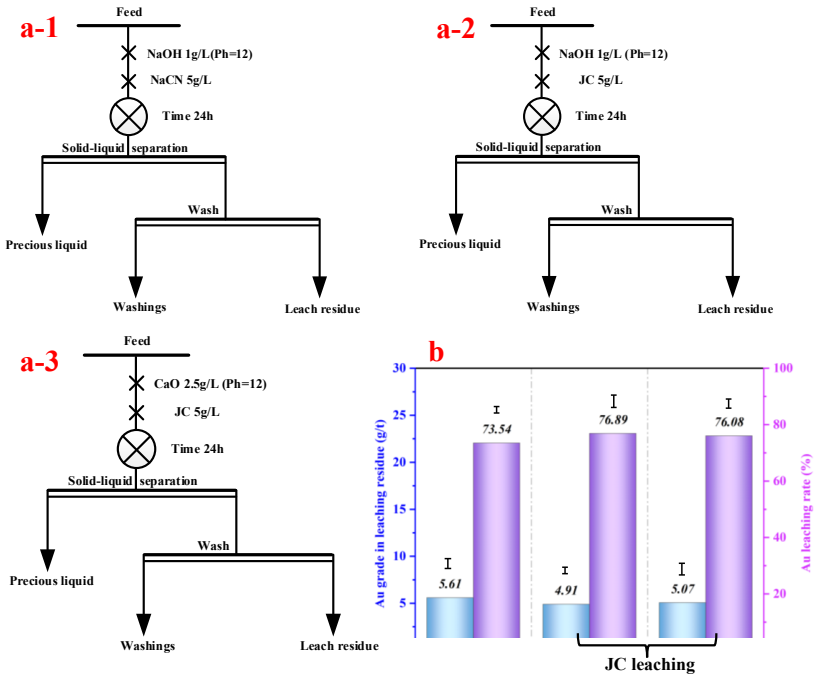

Fig. 7. Direct leaching test process and Direct leaching results; a-1. NaCN direct leaching test (NaOH pulping); a-2. JC leaching test (NaOH pulping); a-3 JC leaching test (CaO pulping); b) Leaching results under three test conditions

Through the above process, the gold leaching rate achieved by direct NaCN leaching was 73.54%. Since the direct leaching rate was below 80%, the gold ore is classified as a refractory gold ore (Mohammadi et al., 2017). It should be noted that the difficult-to-leach classification here mainly reflects the practical status: gold minerals cannot be effectively leached under the experimental conditions. Under the same conditions, the gold leaching rate reached 76.89% using JC for direct leaching. The leaching performance of JC was superior to that of NaCN, and the toxicity of the leaching residue from JC treatment was lower than that from NaCN leaching. From the experimental results, the leaching rate of CaO is 76.08%, which is slightly lower than that of NaOH (76.89%). However, the economic cost of CaO is lower than that of NaOH in practical production and application, so lime was used in the subsequent experiments. It is worth noting that the coarse-grained ore was directly leached, with a gold leaching rate of 76.89%. The proportion of released gold differs by only 0.43% from that of the final extraction, which may be attributed to the dissociation of partially leached gold from limonite and pyrite during the leaching process. Gold chemical phase analysis was conducted on the tailings after CaO slurry JC leaching, and the results are presented in Table 5.

Table 5. Gold chemical phase analysis results

Phase	Free and semi-free natural gold	Carbonate-encapsulated gold	Cu-Pb-Zn sulfides encapsulates gold	Limonite-encapsulated gold	Quartz and silicates encapsulated gold	Pyrite-encapsulated gold	Total
Concentration (g/t)	0.11	0.02	0.01	4.76	0.13	0.04	5.07
Relative content (%)	2.17	0.39	0.20	93.89	2.56	0.79	100

The results in Table 5 demonstrate that the gold content in the tailings is 5.07 g/t, in which limonite-encapsulated gold accounts for as high as 93.89%, whereas free and semi-exposed native gold constitutes only 2.17%. Combined with the process mineralogy results of the raw ore, the main reasons responsible for the low direct leaching rate can be summarized as the following three points:(1) The particle size of native gold is fine, mainly distributed between 0.01 mm and 0.5 mm, and fine grinding is required to achieve monomer dissociation. (2) Gold is closely associated with limonite. The proportion of gold encapsulated in limonite is 23.18% in the raw ore, whereas it increases to 93.89% in the leaching tailings. This indicates that conventional leaching fails to efficiently recover gold hosted in limonite, and pretreatment or enhanced liberation is necessary to improve gold recovery. (3) Some intergranular gold and fissure gold are closely related to pyrite and occur as inclusions, which are difficult to fully expose and leach under conventional leaching conditions. In summary, JC exhibits a favorable effect on the recovery of easily exposed gold. However, for encapsulated gold mainly hosted in limonite, further optimization of process conditions or the introduction of pretreatment measures is still required.

5.1.2. Grinding fineness test results

Grinding fineness tests were conducted to achieve the complete dissociation of gold particles, thereby enhancing the gold leaching rate. With all other conditions kept constant, grinding fineness was set as the sole variable, and the adopted experimental procedure was designated as the gold regrinding–JC leaching process. The schematic of this procedure is illustrated in Fig. 8a, and the corresponding experimental results are presented in Fig. 8b.

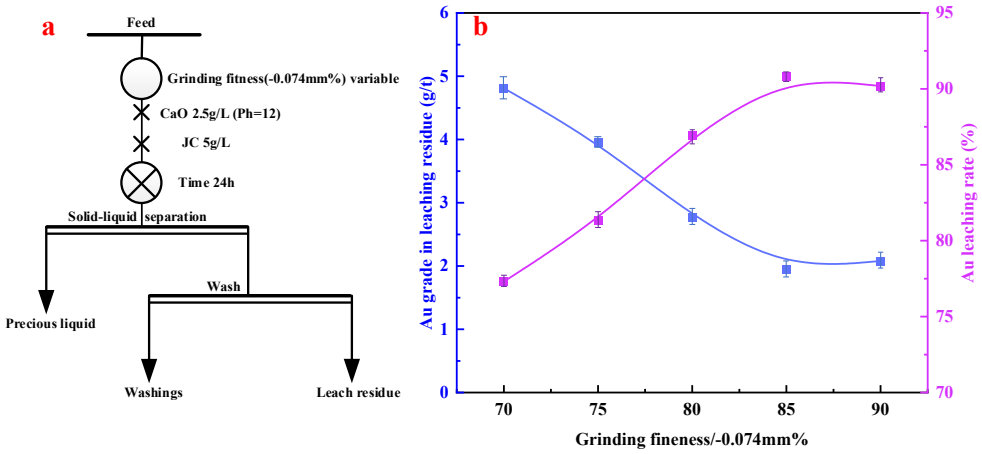

Fig. 8. a) Grinding fineness test process; b) Grinding fineness results

As can be seen from Fig. 8b, the gold grade in the leaching tailings gradually decreases with an increase in the proportion of particles finer than 200 mesh (−0.074 mm), whereas the gold leaching rate exhibits a corresponding gradual increase. This trend indicates that an increase in grinding fineness enhances the degree of monomer dissociation, thereby significantly boosting the leaching rate. When the grinding fineness of −0.074 mm particles reach 85%, the gold leaching rate is as high as 91.16%. Compared with the aforementioned direct leaching test, the leaching rate is increased by approximately 15 percentage points. With a further increase in grinding fineness, the gold leaching rate decreases slightly. This phenomenon may be attributed to severe over-mudding of the ore, which causes ineffective consumption of the leaching reagents. Meanwhile, some gold particles are also encapsulated by the slime, thereby reducing the leaching efficiency. Therefore, the optimal grinding fineness is determined to be 85% passing −0.074 mm.

5.1.3. Leaching agent dosage test results

A non-cyanide lixiviant was employed as the leaching agent in this experiment. The procedure for the lixiviant dosage test is illustrated in Fig. 9a, and the corresponding test results are presented in Fig. 9b.

As can be seen from Fig. 9b of the test results, the gold leaching rate increases with the increase in the dosage of the leaching agent. When the leaching agent dosage reaches 5 g/L, the gold leaching rate

nearly reaches a plateau. Further increasing the leaching agent dosage fails to improve the gold leaching rate significantly. This is because a portion of the gold in the ore exists in the form of lattice-substituted gold, which is scarcely amenable to leaching via conventional methods. Thus, the optimal dosage of the leaching agent is determined to be 5 g/L.

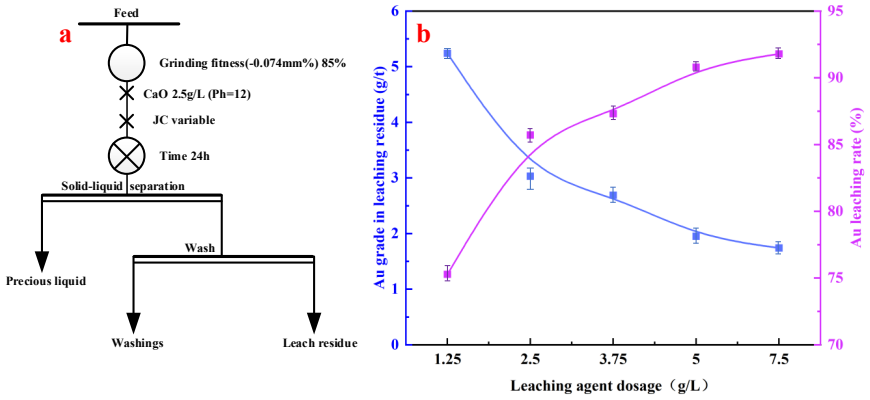

Fig. 9. a) Leaching agent dosage test process; b) Leaching agent dosage test results

5.1.4 Leaching pH test results

With all other experimental conditions kept constant, this study investigated the effect of pH on gold leaching efficiency during the leaching process, using pH as the sole variable. The experimental procedure is illustrated in Fig. 10a, and the corresponding results are presented in Fig. 10b.

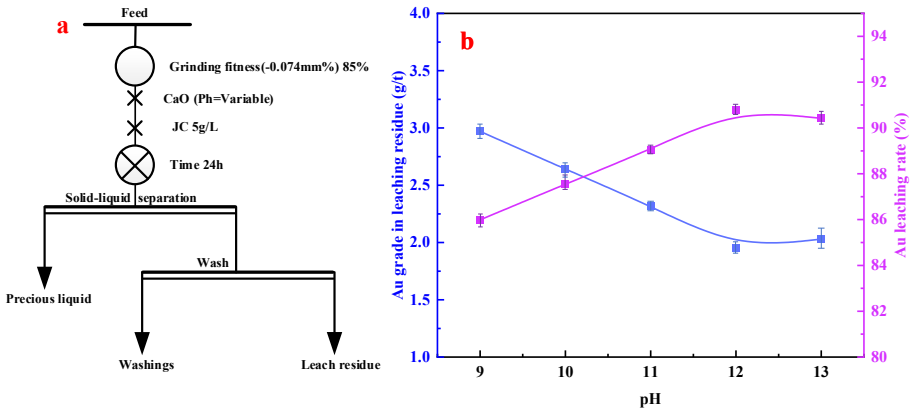

Fig. 10. a) Leaching pH test process; b) Leaching pH test results

As indicated by the results in Fig. 10b, when the lime dosage was set at 0.5, 1, 1.5, 2.5 and 3.5 g/L, the corresponding pH values were 9, 10, 11, 12 and 13, respectively. As the lime dosage increased, the gold leaching rate exhibited a corresponding increase. At a lime dosage of 2.5 g/L (i.e., a pH of 12), the gold leaching rate reached 90.80%, with the grade of the leaching residue being 1.95 g/t. On this basis, the optimal lime dosage is recommended to be 2.5 g/L, corresponding to a recommended pH value of 12.

5.1.5. Leaching time test results

With all other conditions kept constant, a series of experiments were conducted to determine the optimal leaching time. The experimental procedure is illustrated in Fig. 11a, and the corresponding results are presented in Fig. 11b.

The test results are presented in Fig. 11b. The experimental data demonstrate that extending the leaching time facilitates an increase in the gold leaching rate. Specifically, the gold leaching rate rose sharply with increasing leaching time and stabilized at 36 h. At this point, the gold leaching rate reached 92.69%, while the gold grade of the leaching tailings was measured at 1.55 g/t. Further extension of the

leaching time induced no significant variation in the gold leaching rate. Therefore, based on a comprehensive consideration, the optimal leaching time was determined as 36 h.

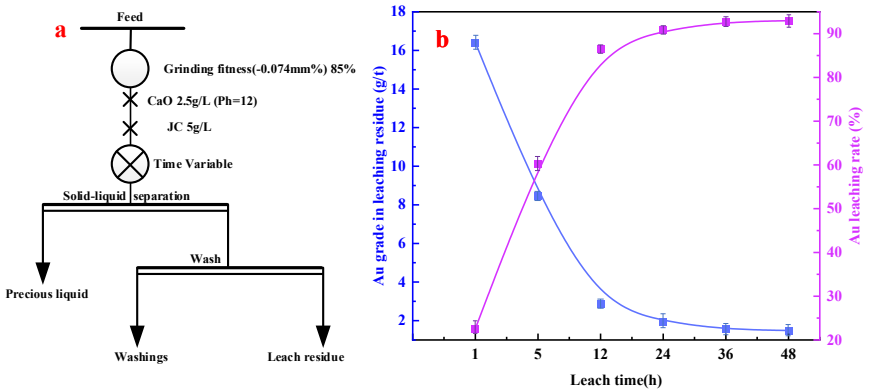

Fig. 11. a) Leaching time test process; b) Leaching time test results

5.2. Leaching aid agent test results

5.2.1. Leaching aid agent type test and results

Under the optimal leaching conditions, the gold leaching rate reached 92.69%, yet the gold grade of the leaching tailings remained as high as 1.55 g/t. To maximize gold recovery, a leaching aid was introduced during the leaching process, aiming to enhance the gold leaching rate and reduce the gold grade of the tailings. Leaching aids for gold leaching are mainly classified into four categories: oxides, ammonium salts, heavy metal salts and organic compounds. Under the experimental conditions of a grinding fineness where particles smaller than 0.074 mm accounted for 85%, a liquid-to-solid ratio of 4:1, pulp pH adjusted using 2.5 g/L of CaO, a JC dosage of 5 g/L, and mechanical stirring at a speed of 500 r/min, H_2O_2, $KMnO_4$, NH_4Cl, $Pb(NO_3)_2$, EDTA, and $C_6H_8O_7$ were added to pretreat the pulp for 2 h. At this stage, the dosages of the above leaching agents correspond to the optimal values under the experimental conditions. The test procedure is illustrated in Fig. 12a, and the test results are presented in Fig. 12b.

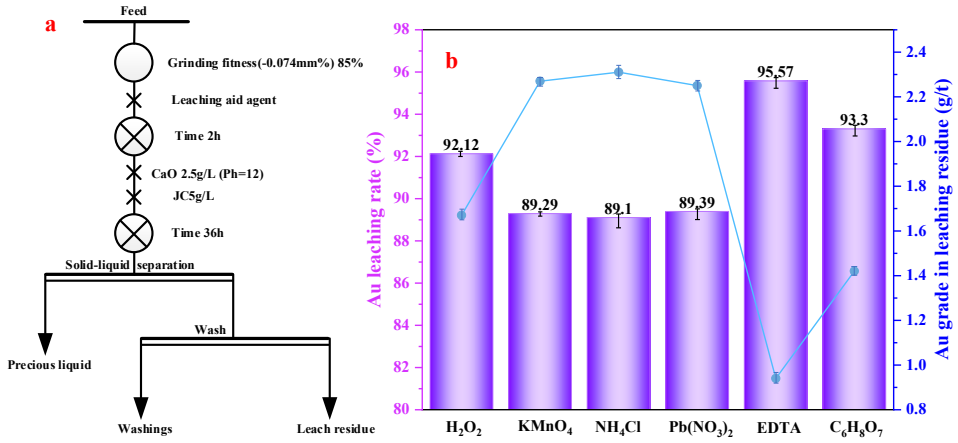

Fig. 12. a) Leaching aid agent type test process; b) Leaching aid agent type test results

Fig. 12b presents the corresponding test results. In comparison with the leaching trial without any leaching aids (where the gold grade in the leaching residue was 1.55 g/t and the leaching rate reached 92.69%), the addition of H_2O_2, $KMnO_4$, NH_4Cl and $Pb(NO_3)_2$ failed to reduce the gold grade in the leaching residue, and thus could not enhance the gold leaching rate. It is worth noting that the chelating leaching aids EDTA and sodium citrate ($C_6H_5Na_3O_7$) were first employed for the pretreatment of the gold ore. Subsequent leaching tests demonstrated that the gold leaching efficiency was significantly enhanced, with EDTA exhibiting the optimal performance. Specifically, the gold leaching rate reached

95.57%, and the gold grade of the leaching tailings was only 0.94 g/t. By comparison, sodium citrate ranked second in terms of leaching efficacy, achieving a gold leaching rate of 93.30% and a tailings gold grade of 1.42 g/t.

It should be acknowledged that when comparing different Leaching aid under identical conditions, the chemical environment for each reagent cannot be individually optimized, including pH and redox potential. Nevertheless, this parallel comparison offers a practical and easy-to-implement basis for preliminary performance screening, and is particularly valuable for industrial applications prioritizing process simplicity.

5.2.2. Mechanism analysis of different leaching effect of leaching aid on gold

Process mineralogy analysis revealed that exposed and semi-exposed gold accounted for 76.46%, whereas gold encapsulated by limonite made up 23.18%. Limonite is a complex; hydrous iron oxide mixture formed via the chemical weathering of iron-bearing minerals under surface environmental conditions. Generally, for gold occluded within different types of limonite, appropriate leaching aids must be selected from the perspective of process mineralogy. Different leaching aids also exhibit distinct leaching performances during the leaching process. This phenomenon can be attributed to the different interaction mechanisms between various leaching aids and JC under strongly alkaline leaching conditions. For example, although oxygen, H_2O_2, and $KMnO_4$ possess certain oxidation capacity under alkaline conditions (Bao et al., 2021; Hu et al., 2026), they may compete with the active components in JC or cause over-oxidation during leaching. Such effects not only reduce the gold leaching efficiency of JC but also inhibit gold dissolution. Ammonium salts and heavy metal salt leaching aids exhibit limited leaching performance because they tend to form precipitates or undergo morphological changes in high-pH environments (García et al., 2025; He et al., 2026). In contrast, the mechanism of chelating leaching aids (EDTA and citric acid (CA)) is more synergistic with JC: these reagents can efficiently complex metal cation impurities in the pulp, remove the oxide film coating the surfaces of gold particles, thereby creating a cleaner and more stable reaction interface for JC and significantly enhancing the gold dissolution efficiency (Abdimomyn et al., 2025; Li et al., 2025; Li et al., 2025; Yan et al., 2025). Therefore, in an alkaline environment-friendly leaching system, chelation exhibits greater advantages over direct oxidation or precipitation by means of optimizing the leaching environment, thus achieving the optimal leaching performance.

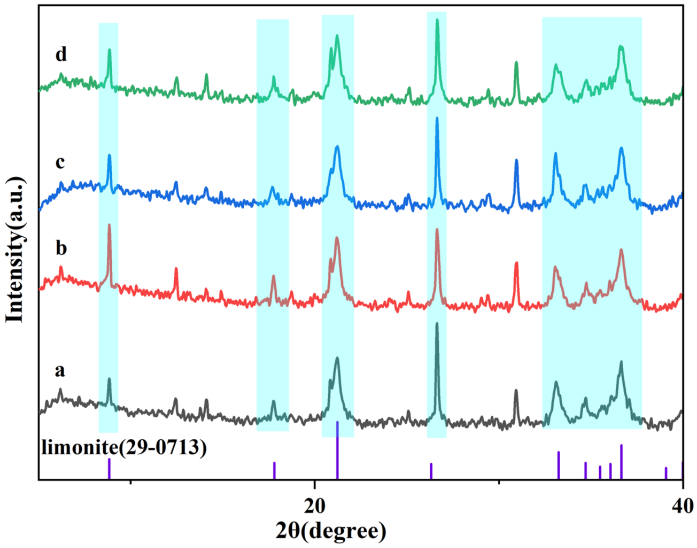

Fig. 1. a) XRD of raw ore; b) XRD of tailings in direct leaching test; c) XRD of tailings without EDTA leaching test; d) XRD of tailings after EDTA pretreatment leaching test

CA as a tridentate organic acid, it can form moderately stable, water-soluble complexes with a variety of metal ions (e.g., Fe^{3+}, Cu^{2+}, Pb^{2+}, Zn^{2+}), thereby transferring metals from the solid phase to the liquid phase. This effect is particularly pronounced for oxides, carbonates and certain sulfide oxidation products (Bhagaskara et al., 2026; Xing et al., 2025). CA exerts its optimal performance in an

environment with a pH < 6. It was concluded from the aforementioned tests that the pulp pH after ore fine grinding was approximately 8, which is alkaline. Although CA exhibited a positive effect on enhancing the leaching rate in the leaching agent type test, the optimal leaching pH in the subsequent leaching tests was 12 (strongly alkaline). In addition, the leaching efficiency after pretreatment with EDTA was superior to that with CA. Therefore, EDTA was selected as the leaching agent for subsequent tests. XRD (Fig. 13) and SEM-EDS (Fig. 14) were used to perform phase identification, microstructure observation, and elemental analysis on the tailings obtained from direct leaching, non-EDTA leaching, and leaching after EDTA pretreatment.

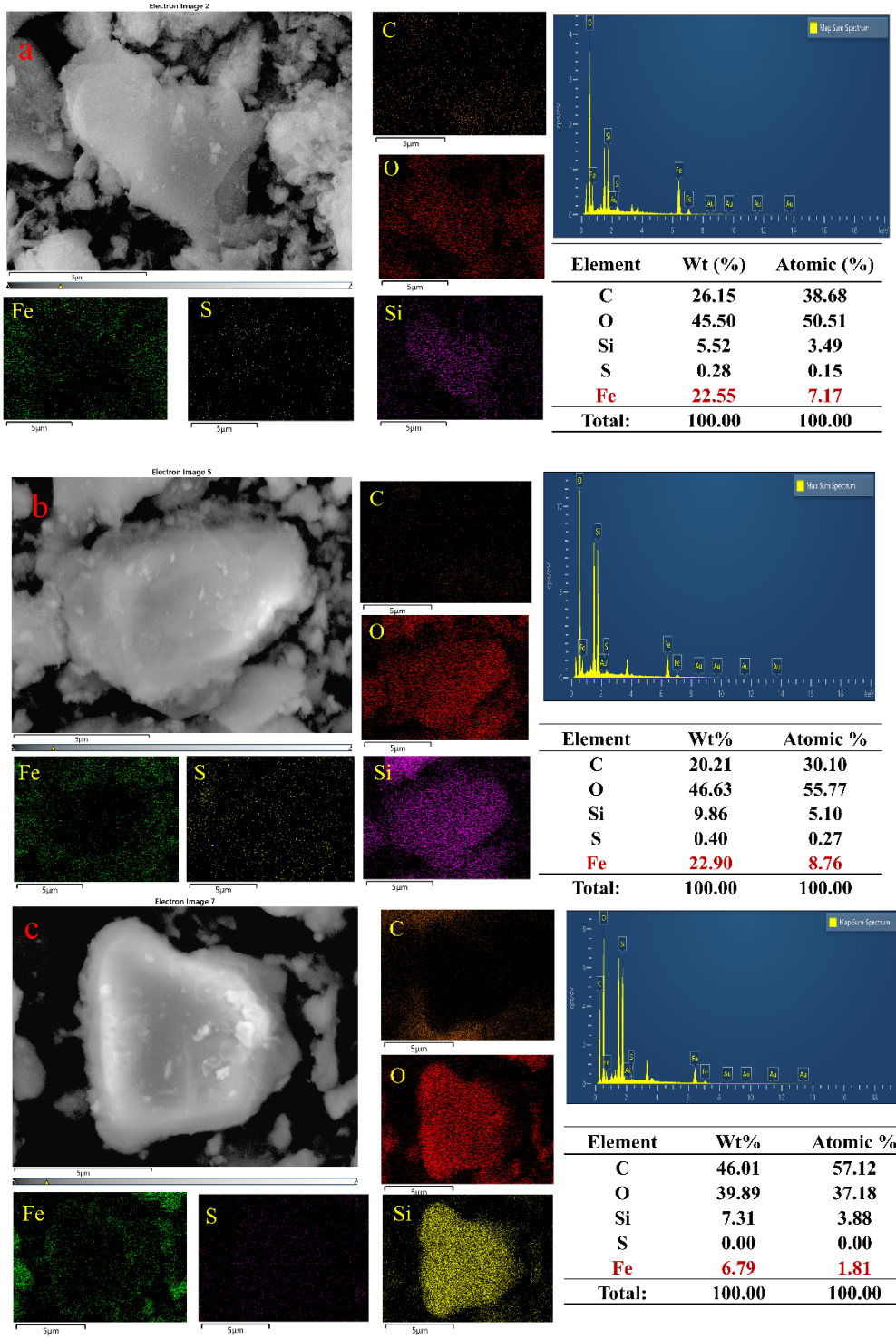

Fig. 2. a) SEM-EDS of tailings in direct leaching test; b) SEM-EDS of tailings without EDTA leaching test; c) SEM-EDS of tailings after EDTA pretreatment leaching test

XRD analysis shows that the characteristic peak of limonite in the raw ore (a) is distinct, which is consistent with the conclusion from process mineralogy research that gold occurs mainly as inclusions within limonite. In the direct leaching test (b), the limonite peak in the XRD pattern of the tailings remains strong, indicating that limonite has not been effectively decomposed and gold remains encapsulated. This is consistent with the lowest leaching rate (76.08%) and the higher iron content (22.55%) observed by EDS. In the EDTA-free leaching test (c), the limonite peak of the tailings was slightly weakened, indicating that a portion of limonite was dissociated and gold was partially liberated. Correspondingly, the leaching rate increased to 92.69%. However, EDS showed that the iron content in the residue remained high (22.90%), demonstrating that limonite was not completely dissociated. After EDTA pretreatment, the limonite peak in the XRD pattern of the leaching test (d) tailings was significantly weakened. EDS analysis showed that the iron content in the slag decreased to 6.79%, which demonstrated that EDTA could effectively destroy the limonite structure via iron ion complexation, thereby fully liberating encapsulated gold and increasing the gold leaching rate to 95.57%.

EDTA possesses strong chelating capacity and can form stable complexes with most multivalent heavy metal ions in aqueous solutions. Numerous researchers have reported that EDTA can dissolve the oxidation products of sulfide ores during the flotation process of such ores. The underlying mechanism is that during leaching, the strong chelating ability of EDTA stems from its multidentate ligand structure, which enables it to form highly stable and water-soluble complexes with target metal ions (Marmier et al., 2025; Wan et al., 2024). This is proposed to effectively disrupt the chemical bonds and lattice bindings of metals in solid phases (e.g., oxides, carbonates, hydroxides, or partial sulfide oxidation products), thereby facilitating the transfer of metal ions from the solid phase to the liquid phase. The leaching-promoting mechanism is proposed to involve two key steps: first, free or complexed EDTA rapidly adsorbs onto the active sites of the mineral surface via surface coordination, potentially weakening and disrupting the metal-oxygen (Me-O) bonds; subsequently, the metal ions dissociate from the mineral lattice and migrate into the solution. This interpretation is consistent with the observed reduction in iron content and the weakening of limonite XRD peaks. Meanwhile, the presence of EDTA may contribute to the destruction or removal of the surface oxide layer, which could expose a fresh gold surface. Further surface analysis is required to verify this mechanism. This is suggested to expose the reactive mineral surface within the oxidized mineral, thereby potentially enhancing the effect of the subsequent leaching agent and further improving the leaching rate and recovery rate of the target metal. Therefore, it is proposed that EDTA can act not only as an efficient chemical complexing leaching agent in the aforementioned leaching process, but also as a key surface activation and pretreatment agent. By synergistically regulating the dissolution equilibrium and surface reaction pathway, selective and enhanced leaching of the target metal is achieved.

To investigate the application of this method in practical engineering, we performed preliminary tests on EDTA dosage and pretreatment time, aiming to determine the optimal conditions for this type of lateritic gold deposit and provide a reliable reference for industrial applications.

5.2.3. EDTA dosage test results

The effect of EDTA dosage on gold leaching was investigated under the following leaching conditions: grinding fineness with −0.074 mm fraction accounting for 85%, liquid-to-solid ratio of 4:1, pretreatment duration of 2 h, lime dosage of 2.5 g/L for pulp pH adjustment, JC dosage of 5 g/L, and mechanical stirring at 500 r/min for 36 h. The corresponding test results are presented in Fig. 15a. As can be seen from Fig. 15a, the gold leaching rate increases first and then decreases with an increase in EDTA dosage. When the EDTA dosage reaches 0.25 g/L, the gold leaching rate attains its maximum value (95.57%); beyond this dosage, the leaching rate declines continuously. This trend arises from multiple factors. For instance, as the EDTA concentration rises, it complexes with the active components of the leaching agent in the solution, thereby lowering the leaching efficiency. Accordingly, the optimal dosage of the chelating agent EDTA is recommended as 0.25 g/L.

5.2.4. Pretreatment time test results

The effect of pretreatment time on gold leaching was investigated under the following leaching conditions: grinding fineness of −0.074 mm with 85% passing, a liquid-to-solid ratio of 4:1, an EDTA dosage of 0.25 g/L, lime dosage of 2.5 g/L to adjust the pulp pH, a JC dosage of 5 g/L, and mechanical

stirring at 500 r/min for 36 h. The test results are presented in Fig. 15b. When the leaching time was increased from 1 h to 24 h, the gold leaching rate increased with the extension of the pretreatment time. At pretreatment times of less than 12 h, the leaching rate rose in tandem with the extension of leaching time. Specifically, a leaching rate of 97.17% was achieved at a pretreatment time of 12 h, whereas a leaching rate of 97.41% was obtained at 24 h of pretreatment. It can be concluded that prolonging the pretreatment time did not yield a significant improvement in the leaching rate. Therefore, 12 h was selected as the optimal pretreatment duration for subsequent tests.

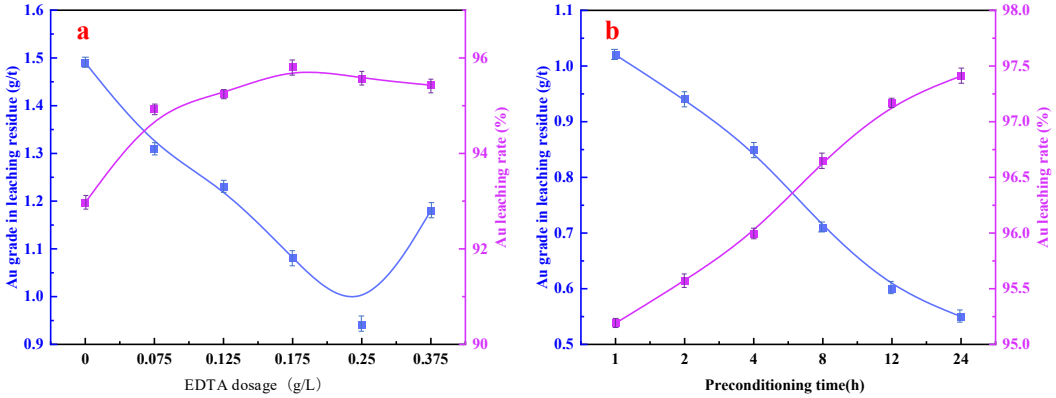

Fig. 15. a) EDTA dosage test results; b) Pretreatment time test results

5.2.5. Preliminary exploration test of process flow

Under the optimum leaching conditions of a grinding fineness of 85% −0.074 mm, a liquid-solid ratio of 4:1, EDTA concentration of 0.25 g/L, pretreatment time of 12 h, pulp pH of 12, JC dosage of 5 g/L, and mechanical stirring at 500 r/min for 36 h, gold recovery from the leachate was investigated. The flow chart is shown in Fig. 16, and the results are presented in Table 6.

The results of exploratory experiments show that, the leaching rate of gold in the leaching stage reached 97.17%, while the total gold recovery throughout the entire process stood at 95.59%. The gold grade of the activated carbon was 946.00 g/t, indicating an excellent gold recovery performance. These results suggest that the optimized recovery process exhibits favorable industrial feasibility and application potential under the optimal experimental conditions and offer rational and innovative technical insights for industrial practitioners.

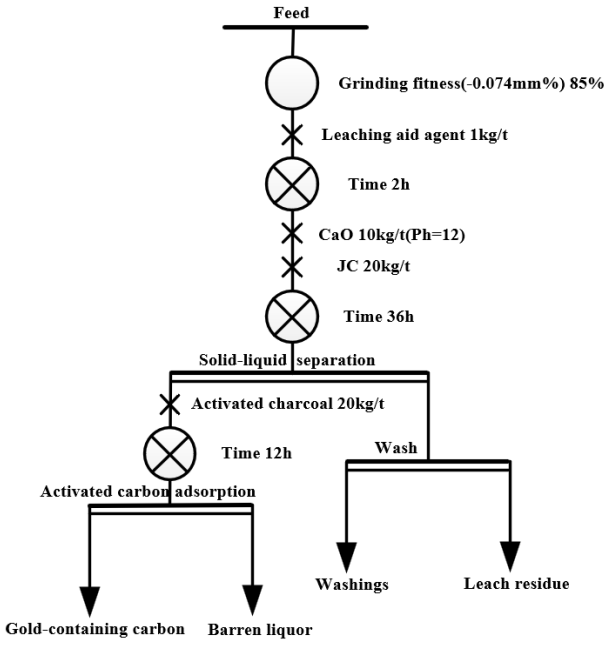

Fig. 16. Exploration test process of gold recovery

Table 6. Exploration test results of gold recovery

Gold leaching		Gold grade after adsorption (mg/L)	0.08
Grade of leached dust (g/t)	0.60	Gold grade before adsorption (mg/L)	4.91
Feed grade (g/t)	21.20	adsorption rate (%)	98.37
Leaching rate of slag (%)	97.17	Gold grade in activated carbon(g/t)	946.00

6. Conclusions

(1) Process mineralogy studies show that the lateritic gold ore contains 42.60% iron and 21.20 g/t gold, indicating a high comprehensive recovery value. Gold occurs primarily as bare and semi-bare native gold (76.46%) and gold encapsulated in limonite (23.18%). It exhibits a fine-grained dissemination texture and is closely associated with limonite and pyrite.

(2) Direct leaching with the environment-friendly lixiviant JC yields a gold leaching rate of only 76.89%, confirming that the ore is a typical refractory gold ore. Through systematic optimization, a "fine grinding-JC leaching-EDTA leaching-activated carbon adsorption" process was determined as the appropriate flow sheet. The optimum conditions are as follows: grinding fineness of 85% passing 0.074 mm, EDTA dosage of 0.25 g/L for a 12-h pretreatment, JC dosage of 5 g/L, lime addition to maintain pH at 12, and leaching time of 36 h. Under these conditions, the gold leaching rate increases to 97.17%, while the gold grade of the tailings decreases to 0.60 g/t.

(3) EDTA exhibited a significant promoting effect as a chelating leaching aid, with the optimal gold leaching performance achieved at a dosage of 0.25 g/L. The mechanism analysis shows that EDTA may improve the leaching rate of gold by complexing surface metal ions and stripping oxide layer. Subsequent activated carbon adsorption tests demonstrated a gold adsorption rate of 98.37% in the pregnant leach solution, resulting in an overall gold recovery of 95.59% and thus achieving efficient and clean recovery.

(4) This study successfully constructed an environment-friendly leaching system suitable for high-iron, refractory lateritic gold ores. This work provides a technical basis and process design for the industrial application of non-cyanide gold extraction technology to similar resources.

Acknowledgments

The authors are grateful to Prof. Xie (Kunming University of Science and Technology) for his valuable suggestions and insightful discussions. We also sincerely appreciate the assistance provided by the members of his research group during the experimental and analytical phases of this work.

References

ABDIMOMYN, S., ZHANATKYZY, Z., ARTUR, G., MALIK, S., ZHUMADIL, K., NECHIPURENKO, S., & MALCHIK, F. J. R. A. ,2025. *Citrate-EDTA-H_2O_2 buffering leaching solution for Ni/Co/Mn recovery from spent lithium-ion battery black mass.* RSC Advances .15(48), 40864-40882.

BAO, J., LI, K., NING, P., WANG, C., SONG, X., LUO, Y., & SUN, X. J. J. O. E. S. ,2021. *Study on the role of copper converter slag in simultaneously removing SO_2 and NO_x using KMnO4/copper converter slag slurry.* Journal of Environmental Sciences .108, 33-43.

BHAGASKARA, A., SAPUTRA, D. A., TRISUNARYANTI, W., WIJAYA, K., ROZANA, K., SUSANTO, H., . . . PRASETYO, A. B. J. J. O. T. I. C. S. ,2026. *Investigation of Reaction Mechanism in Selective Citric Acid Leaching of Ni and Co from NMC Cathodes via Real Time Raman Spectroscopy and RSM Optimization.* Journal of the Indian Chemical Society. 102410.

GARCÍA, N. M., MARTINEZ, J. G., VALVERDE, J. L., CANO, B. D., HUOT, J., HEITZ, M., 2025. *Selective zinc recovery from spent alkaline batteries via multistage leaching with ammonium salts.* Cleaner Engineering and Technology. 24, 100863.

GUO, X.-Y., LIU, Z.-W., TIAN, Q.-H., LI, D., & ZHANG, L. J. H. ,2022. *Gold extraction from Carlin-type concentrate by a novel environmentally friendly lixiviant.* Hydrometallurgy.211, 105884.

HAO, J., WANG, X., WANG, Y., GUO, F., & WU, Y. J. H.,2023. *Study of gold leaching from pre-treated waste printed circuit boards by thiosulfate-cobalt-glycine system and separation by solvent extraction.* Hydrometallurgy.221, 106141

HE, B., WANG, J., LIU, Y., ZHANG, R., LIU, H., YANG, B., FANG, Y. J. M. E.,2026. *Citric acid composite ammonium salt-efficient leaching ion-adsorption rare earth ore.* Minerals Engineering.237, 110042.

HOU, L., VALDIVIESO, A. L., ROBLEDO-CABRERA, A., ZAINIDDINOVICH, N. Z., WU, C., SONG, S., & JIA, F. J. P. T. ,2024. *Stepwise oxidation of refractory pyrite using persulfate for efficient leaching of gold and silver by an eco-friendly copper (II)-glycine-thiosulfate system.* Powder Technology.448, 120323.

HILSON, G., & MONHEMIUS, A. J. J. O. C. P. ,2006. *Alternatives to cyanide in the gold mining industry: what prospects for the future?* Journal of Cleaner production.14(12-13), 1158-1167.

HU, Y., XU, J., ZHANG, F., TIAN, Y., & REN, Y. J. M. E. ,2026. *Leaching kinetics of precious metals from platinum–palladium concentrate using H2O2 in an acidic chloride system.* Minerals Engineering.237, 110031.

IGLESIAS-MARTÍNEZ, M., SALAMA, W., ANAND, R. R., BUTT, C. R., & ESPÍ, J. A. J. O. G. R. ,2024. *Exploration and mining of lateritic gold deposits (Part I): Ore formation, characterization, and sampling of ferruginous gravel and duricrust.* Ore Geology Reviews. 170, 106146

LI, J., TONG, L., ZHANG, H., CHEN, Q., YANG, H., SHEN, L., YAO, R. J. G. C. E. ,2024. *Pool bio-oxidation and fitting analysis of low-grade arsenic-containing refractory gold ore.* Green Chemical Engineering. 5(4), 511-518.

LI, S., CHEN, Q., CAO, Z., CHEN, J., YANG, J. J. C., PHYSICOCHEMICAL, S. A., & ASPECTS, E. ,2025. *Investigation into aluminum leaching from vein quartz in a calcium fluoride-enhanced citric acid-tartaric acid system.* Colloids and Surfaces A: Physicochemical and Engineering Aspects. 709, 136189.

LI, Y., DONG, L., LI, B., LI, Y., SHI, P., YANG, H., ZHOU, Z. J. C. E. S. ,2025. Selective recovery of neodymium from NdFeB wastes by chlorinated roasting and citric acid leaching. Chemical Engineering Science. 307, 121351.

LIU, X., CHEN, Y., HU, Y., LIANG, J., WANG, Y., HE, W., & CHEN, X. J. J. O. G. E. ,2023. *Fine gold grains inside the limonite in the supergene Shangmanggang gold deposit, SW China: Implications for gold mobilization and mineral exploration.* Journal of Geochemical Exploration. 248, 107193.

MA, T., CHEN, C., ZHANG, Y., YANG, Y., LIU, X., LAI, X., FAN, T. J. O. G. R. ,2024. *Mineralogy and mineral chemistry of Bi-Te minerals: Constraints on mineralization process of the Dulanggou gold deposit, Dadu River Metallogenic Belt, China.* Ore Geology Reviews. 169, 106091.

MA, Y., LI, Q., ZHANG, Y., LIU, X., YANG, Y., JIANG, T. J. S., & TECHNOLOGY, P. ,2025. *A potential strategy for eco-friendly and efficient copper recovery: Ferricyanide-enhanced glycine leaching of copper.* Separation and Purification Technology. 358, 130280.

MARMIER, V., PLANTE, B., DEMERS, I., & BENZAAZOUA, M. J. J. O. G. E. ,2025. *The use of EDTA leaching method to predict arsenic and antimony Neutral Mine Drainage from the Eleonore tailings.* Journal of Geochemical Exploration. 273, 107734.

MOHAMMADI, E., POURABDOLI, M., GHOBEITI-HASAB, M., & HEIDARPOUR, A. J. I. J. O. M. P. ,2017. *Ammoniacal thiosulfate leaching of refractory oxide gold ore.* International Journal of Mineral Processing.164, 6-10.

NAIR, A. V., JAYASREE, S. S., BAJI, D. S., NAIR, S., & SANTHANAGOPALAN, D. J. R. S. ,2024. *Environment-friendly acids for leaching transition metals from spent-NMC532 cathode and sustainable conversion to potential anodes.* RSC Sustainability.2(8), 2377-2388.

NIU, H., YANG, H., & TONG, L. J. J. O. C. P. ,2023. *Research on gold leaching of carbonaceous pressure-oxidized gold ore via a highly effective, green and low toxic agent trichloroisocyanuric acid.* Journal of Cleaner Production.419, 138062.

PENGZHI, G., SHA, Q., & YIPENG, W. J. C. M. M., 2015. *Experimental study on a gold ore in Laos with environment-friendly Jinchan leaching reagents.* China Mining Magazine.24(12), 131-135,141.

SHAFIEI, M., HOSSEINI, M. R., AZIMI, E., & FARNAUD, S. J. I. C. C. ,2025. *Responses of the refractory and free-milling gold ores to chloride leaching as an eco-friendly alternative to the cyanidation method.* Inorganic Chemistry Communications.115104.

SHI, L., MA, B., CAO, Z., YU, J., HE, F., & WANG, C. J. M. E. ,2025. *Environment-friendly and selective extraction of valuable metals from saprolitic laterite via nitric acid pressure leaching: Behavior and mechanism.* Minerals Engineering.227, 109255.

TANG, J., ZHANG, Y., ZI, F., YANG, Z., MU, J. J. J. O. A., & COMPOUNDS. ,2025. *Mechanism of electrochemical oxidation of gold surfaces in a novel cobalt (II)-glycine-thiosulfate leaching system: An electrochemical experiments and DFT study.* Journal of Alloys and Compounds.1010, 177912.

VARAJÃO, C. A. C., COLIN, F., VIEILLARD, P., MELFI, A. J., & NAHON, D. J. A. G. ,2000. *Early weathering of palladium gold under lateritic conditions, Maquiné Mine, Minas Gerais, Brazil.* Applied Geochemistry .15(2), 245-263.

WAN, J., CHEN, Z., LIU, X., TANG, Z., DENG, H. J. S., & INTERFACES. ,2024. *Enhanced heavy metal leaching from volcanic muds: Synergistic effects of citric acid and EDTA composite system.* Surfaces and Interfaces.48, 104287.

XING, B., CHEN, C., XIAN, Y., LIANG, G., WEN, S., CHEN, L., & ZHANG, S. J. P. T. ,2025. *Selective separation of smithsonite from carbonate gangue using citric acid as depressant: An integrated experimental and DFT calculation.* Powder Technology.121631.

YAN, Y., SUN, S., WEI, J., SHUBO, A., XIAO, F., & TU, G. J. M. E. ,2025. *Enhanced sulfuric acid leaching and kinetics of rhodochrosite in the presence of trisodium citrate and EDTA.* Minerals Engineering. 228, 109323.

YOSHIMURA, A., TAKAI, M., & MATSUNO, Y. J. H. ,2014. Novel process for recycling gold from secondary sources: Leaching of gold by dimethyl sulfoxide solutions containing copper bromide and precipitation with water. Hydrometallurgy.149, 177-182.

ZHANG, S., YANG, H., MA, P., LUAN, Z., TONG, L., JIN, Z., & SAND, W. J. M. E. ,2022. *Column bio-oxidation of low-grade refractory gold ore containing high-arsenic and high-sulfur: Insight on change in microbial community structure and sulfide surface corrosion.* Minerals Engineering. 175, 107201.

ZHANG, Y., CUI, M., WANG, J., LIU, X., & LYU, X. J. M. E. ,2022. *A review of gold extraction using alternatives to cyanide: Focus on current status and future prospects of the novel eco-friendly synthetic gold lixiviants.* Minerals Engineering.176, 107336.

ZHANG, Y., PENG, Y., GU, X., WANG, Q., SONG, M. J. O., & GEOLOGY, E. R. ,2024. *Ore-forming process of the Xiaoyuzan gold deposit in the Western Tianshan, Northwest China: Constraints from mineralogy and S isotopes of sulfides.* Ore and Energy Resource Geology. 17, 100058.

ZHONG, W., MENG, G., CUI, J., ZHU, X., LUO, S., TAN, W., PROTECTION, E. ,2025. *Catalytic ozonation of cyanide in gold leaching efluent by EDTA-Coir/copper slag: Efficacy and mechanisms.* Process Safety and Environmental Protection.108216.